

5-15-2003

Design and Analysis for Melt Casting Metallic Fuel Pins Incorporating Volatile Actinides: Quarterly Progress Report 2/16/ 03- 5/15/03

Yitung Chen

University of Nevada, Las Vegas, yitung.chen@unlv.edu

Randy Clarksean

University of Nevada, Las Vegas

Darrell Pepper

University of Nevada, Las Vegas, darrell.pepper@unlv.edu

Follow this and additional works at: https://digitalscholarship.unlv.edu/hrc_trp_fuels



Part of the [Metallurgy Commons](#), [Nuclear Commons](#), and the [Nuclear Engineering Commons](#)

Repository Citation

Chen, Y., Clarksean, R., Pepper, D. (2003). Design and Analysis for Melt Casting Metallic Fuel Pins Incorporating Volatile Actinides: Quarterly Progress Report 2/16/03- 5/15/03. 1-11.

Available at: https://digitalscholarship.unlv.edu/hrc_trp_fuels/8

This Report is protected by copyright and/or related rights. It has been brought to you by Digital Scholarship@UNLV with permission from the rights-holder(s). You are free to use this Report in any way that is permitted by the copyright and related rights legislation that applies to your use. For other uses you need to obtain permission from the rights-holder(s) directly, unless additional rights are indicated by a Creative Commons license in the record and/or on the work itself.

This Report has been accepted for inclusion in Fuels Campaign (TRP) by an authorized administrator of Digital Scholarship@UNLV. For more information, please contact digitalscholarship@unlv.edu.

Design and Analysis for Melt Casting Metallic Fuel Pins Incorporating Volatile Actinides

Quarterly Progress Report 2/16/03- 5/15/03

UNLV Transmutation Research Program

Principal Investigator: Yitung Chen
Co-Principal Investigators: Randy Clarksean and Darrell Pepper

Purpose and Problem Statement

An important aspect of the Advanced Fuel Cycle Initiative (AFCI) program is the development of a casting process by which volatile actinide element (i.e., americium) can be incorporated into metallic alloy fuel pins. The traditional metal fuel casting process uses an inductively heated crucible. The process involves evacuation of the furnace. The evacuation of the furnace also evacuates quartz rods used as fuel pin molds. Once evacuated the open ends of the molds are lowered into the melt; the casting furnace is then rapidly pressurized, forcing the molten metal up into the evacuated molds where solidification occurs.

This process works well for the fabrication of metal fuel pins traditionally composed of alloys of uranium and plutonium, but does not work well when highly volatile actinides are included in the melt. The problem occurs both during the extended time period required to superheat the alloy melt as well as when the chamber must be evacuated. The low vapor-pressure actinides, particularly americium, are susceptible to rapid vaporization and transport throughout the casting furnace, resulting in only a fraction of the charge being incorporated into the fuel pins as desired. This is undesirable both from a materials accountability standpoint as well as from the failure to achieve the objective of including these actinides in the fuel for transmutation.

Candidate design concepts are being evaluated for their potential to successfully cast alloys containing volatile actinides. The selection of design concepts has been conducted in close cooperation with ANL staff. The research centers on the development of advanced numerical models to assess conditions that significantly impact the transport of volatile actinides during the melt casting process. The work will include the collection and documentation of volatile actinide properties, development of several conceptual designs for melt casting furnaces, modeling and analysis of these concepts, development of sophisticated numerical models to assess furnace operations, and analysis of these operations to determine which furnace concept has the greatest potential of success. Research efforts will focus on the development of complex heat transfer, mass transfer, and inductive heating models.

Personnel

Principle Investigator:

- Dr. Yitung Chen (Mechanical Engineering)

Co-Principle Investigators:

- Dr. Randy Clarksean (Mechanical Engineering)
- Dr. Darrell Pepper (Mechanical Engineering)

Graduate Students:

- Mr. Taide Tan, M.S. Graduate Student, (Mechanical Engineering)
- Mr. Byarlaga Yarlagadda, M.S. Graduate Student, (Mechanical Engineering)

National Laboratory Collaborators:

- Dr. Mitch Meyer, Leader of Fabrication Development Group, ANL-West
- Dr. Steve Hayes, Manager of Fuels & Reactor Materials Section, Nuclear Technology Division, ANL-West

Management Progress

Budget Issues:

- N/A

Student Issues:

- N/A

Management Problems

No management problem issues at this time.

Technical Progress

Progress continues on the analysis of casting and solidification of the melt into molds. Modeling results for constant pressure casting, which is more realistic, have been obtained and produce physically realistic results for flow that starts, flows, and then eventually stops as it enters the mold. Potential mass transfer modeling features (Lammuir's law for example) are being studied to enhance the capabilities of a mass transfer in a detailed system model. Different parameters are being varied as part of a parametric study to evaluate factors that impact the flow of the melt into the molds. The ability to include the induction heating governing equations as part of an overall system model is being studied and preliminary efforts to include this complex phenomenon as part of a more detailed model are underway. Figure 1 shows the transient solidification process in the mold.

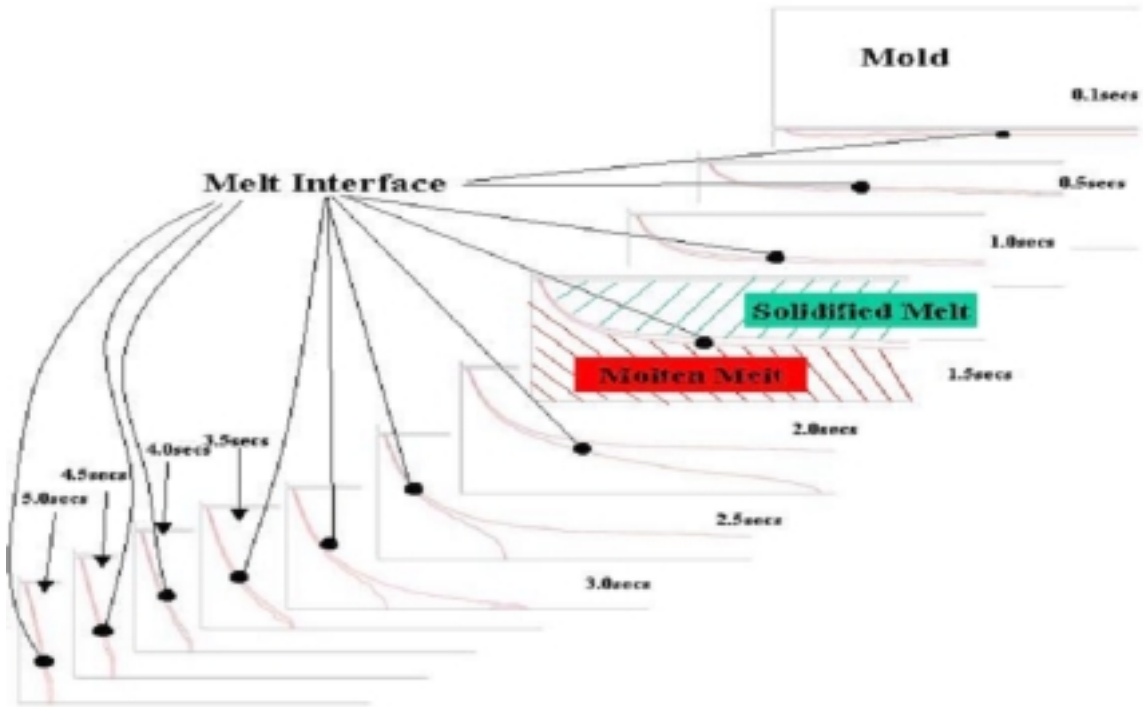


Figure 1. Transient solidification process inside the mold.

The impact of mold preheat temperature and fuel pin diameter on the ability of copper and stainless steel mold to solidify all the molten material for 0.5 m fuel pin have been evaluated which are shown in Figures 2 and 3. Figure 4 shows the non-slip VOF filling processes for the mold casting.

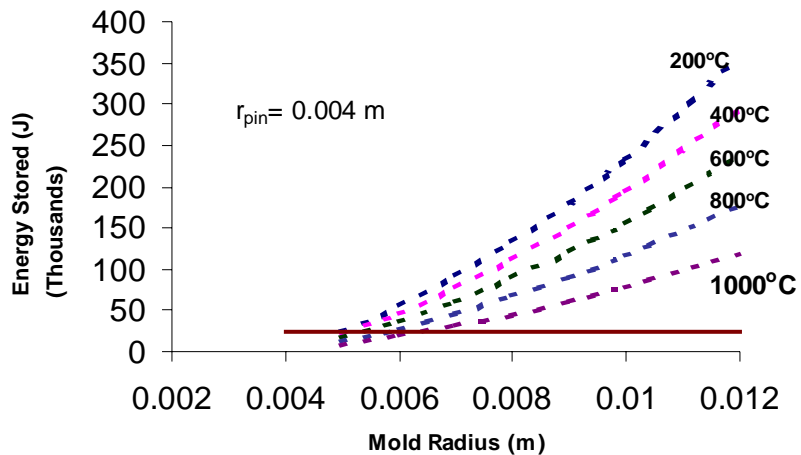


Figure 2. The solidification along with varying mold radius for the different preheat temperature for the specific molten radius of 0.004 m.

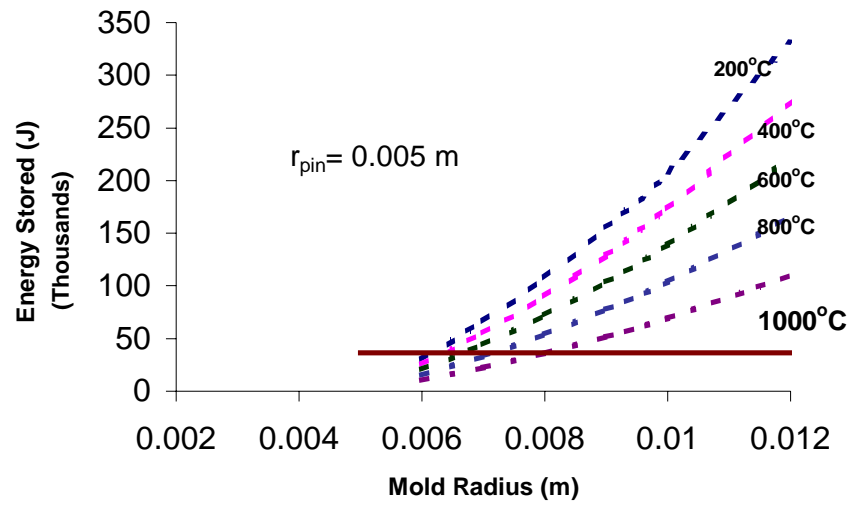


Figure 3. The solidification along with varying mold radius for the different preheat temperature for the specific molten radius of 0.005 m.

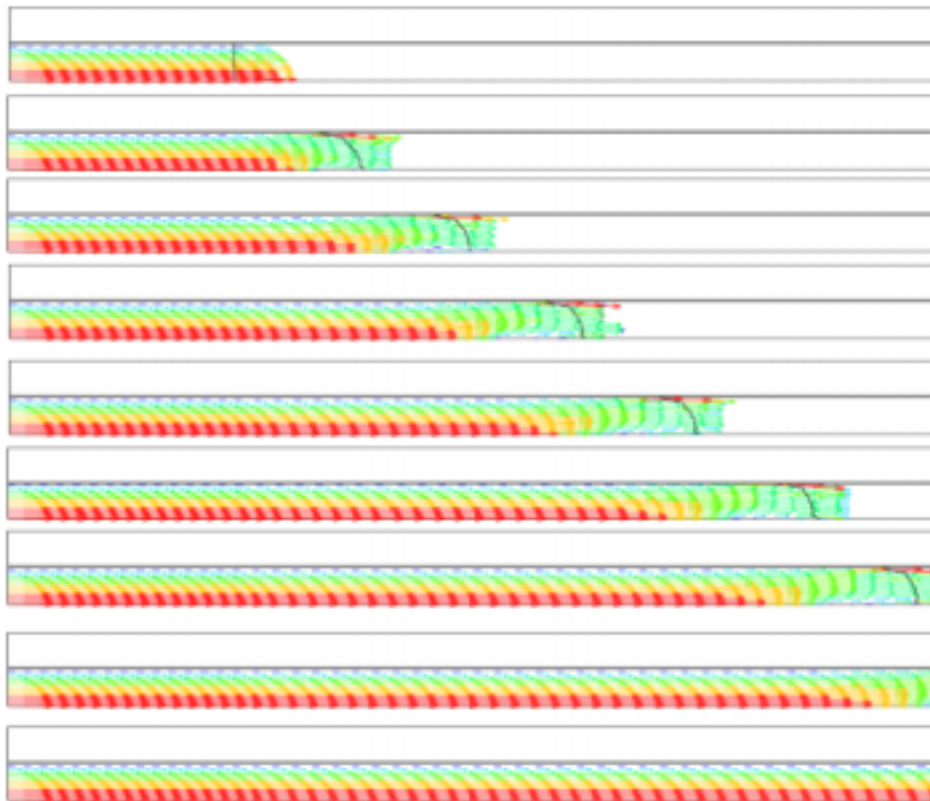


Figure 4. Representative flow field for free surface flow into mold region (axisymmetric geometry shown). Solid line across the velocity vectors represents the fill front.

The solidification processes of constant inlet velocity and constant pressure have also been studied by using different molds preheated temperature, and different inlet pressure. The solidification rates have also been studied which is shown in Figure 5.

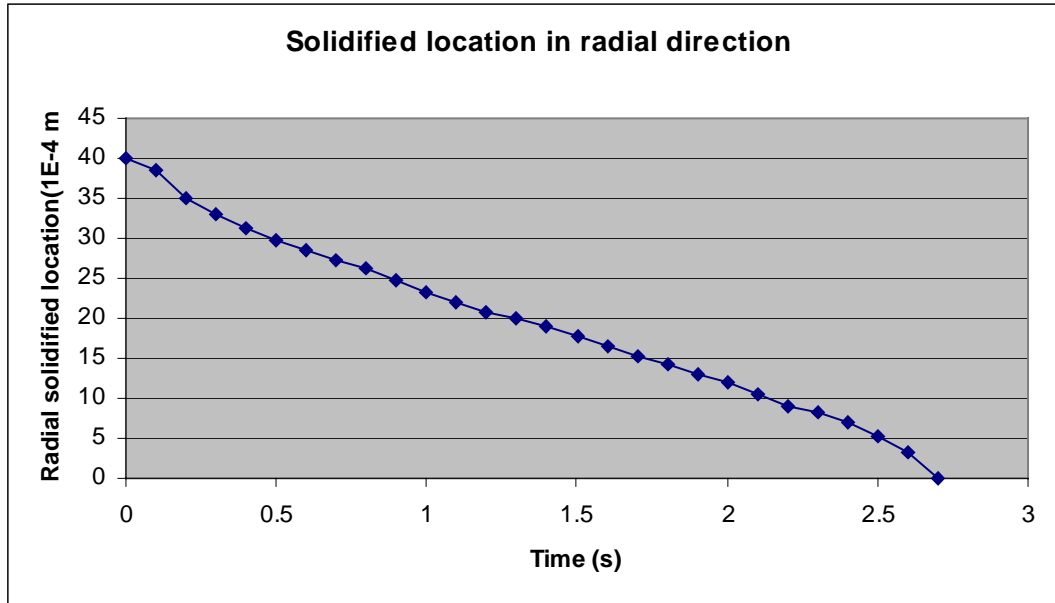


Figure 5. Transient solidified location along the radial direction for copper mold (at $T=1410\text{ }^{\circ}\text{C}$). Boundary conditions and initial conditions: inlet pressure: $P=20\text{ kPa}$; inlet temperature= $1500\text{ }^{\circ}\text{C}$; mold preheated temperature: $T=400\text{ }^{\circ}\text{C}$; convection heat transfer coefficient $h=2000\text{ W/m}^2\text{ }^{\circ}\text{C}$; phase change temperature: $1400\text{-}1410\text{ }^{\circ}\text{C}$

We have also set up the numerical model for the upper part of the casting furnace includes the crucible and coils. The governing equations for the induction heating modeling have also been studied and developed. Figures 6 and 7 show the furnace geometry and the computational mesh. FIDAP was used to solve the induction heating governing equations in order to find the solution of the power deposition rate in the crucible. The calculation of C and S is executed in FIDAP by the species equation (analogy C and S as two special species)

$$\rho_0 \left(\frac{\partial C_n}{\partial t} + \vec{u} \cdot \nabla C_n \right) = \rho_0 \nabla \cdot (\alpha_n \nabla C_n) + q_{cn} + R_n$$

R_n is neglected for the steady state problem. The velocity for the source term R_n is also neglected. Then the equation becomes as follow.

$$\nabla \cdot (\alpha_n \nabla C_n) = -\frac{q_{cn}}{\rho_0}$$

This equation can be related to the six induction heating equations in the same analogy. Once the values of C and S (using FIDAP) are calculated, the power deposition rate is obtained by the following equation.

$$Q(r, Z) = \frac{\sigma \omega^2}{2r^2} (S^2 + C^2)$$

Where in tensor notation the variables S and C in FIDAP are expressed as:
For the coils:

$$\nabla \cdot (K \nabla C) = -\mu J_0$$

$$\nabla \cdot (K \nabla S) = 0$$

For the conductors:

$$\nabla \cdot (K \nabla S) = -\frac{\mu \sigma \omega}{r} C$$

$$\nabla \cdot (K \nabla C) = \frac{\mu \sigma \omega}{r} S$$

For all other locations:

$$\nabla \cdot (K \nabla S) = 0$$

$$\nabla \cdot (K \nabla C) = 0$$

Where:

- K=1/r
- C, S = real and complex components of function
- r = radial coordinate
- J₀ = Current density
- ω = Frequency
- σ = Electrical conductivity
- μ = Permeability (vs/a-m)
- σ = Conductivity (mhos/m)

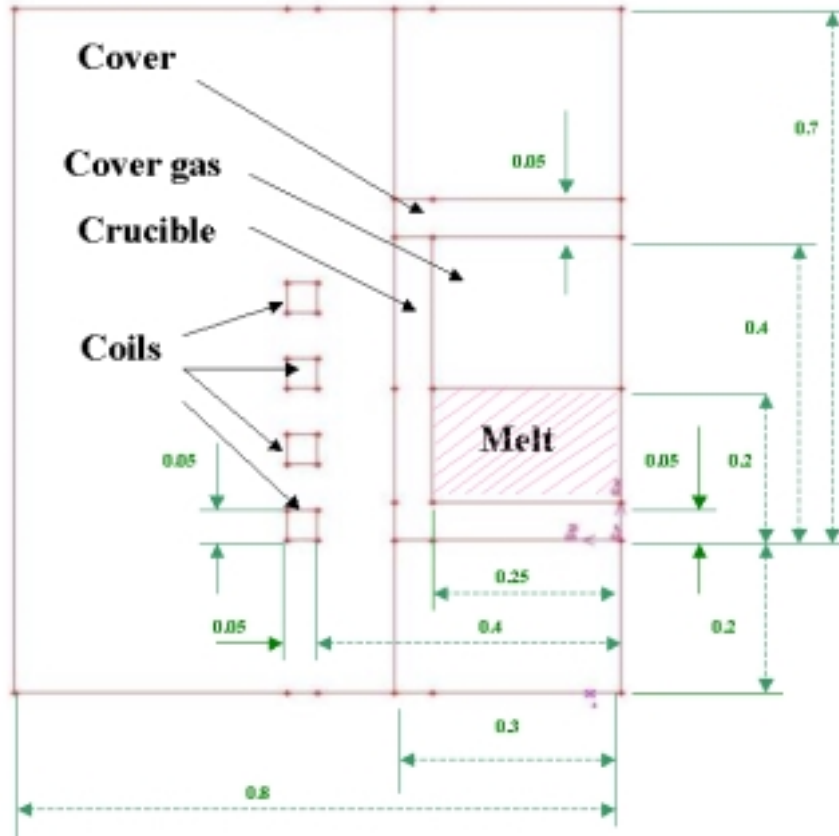


Figure 6. The Geometry of the upper part of the furnace (crucible and coils, unit: m)

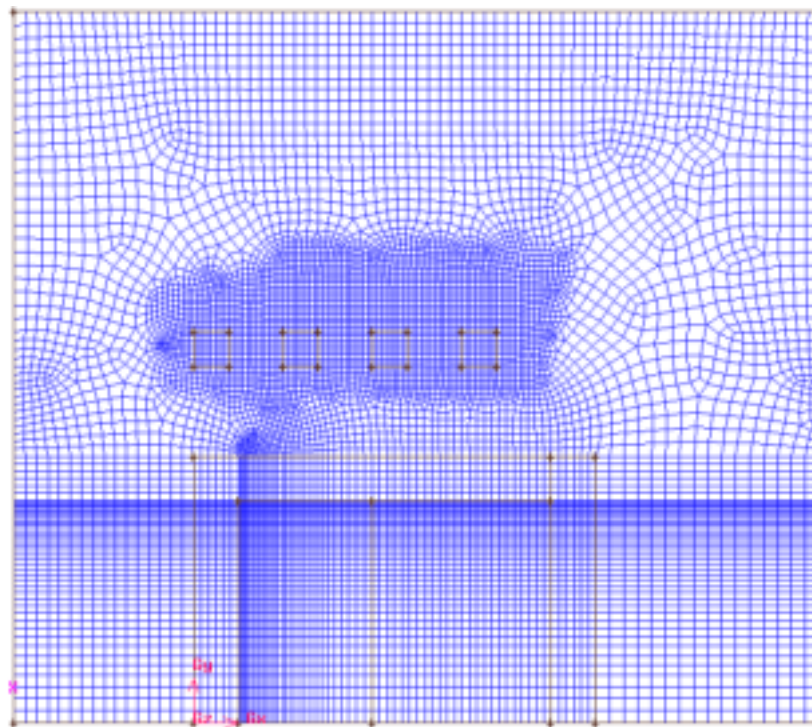


Figure 7. The computational mesh of the furnace.

The changes of the average filling velocity during the solidification process in the molds for different convection heat transfer coefficient have also been analyzed. The solidification process is analyzed at constant filling pressure, $P=20$ kPa. All the other physical properties, initial and boundary conditions are kept as constants. For example, the material of the mold is copper, the mold preheated temperature is 400 °C, initial melt temperature is 1500 °C. The average filling velocity increases rapidly at the beginning of the solidification process till it reaches the maximum value. And then it decreases to zero when the melt is solidified at the centerline of the mold. It is also shown that the entire solidification process with the higher of h value is faster than the lower one. And the minimum of average filling velocity can be found at the highest of h value. Figure 8 shows the comparison of average filling velocity for different heat transfer coefficients.

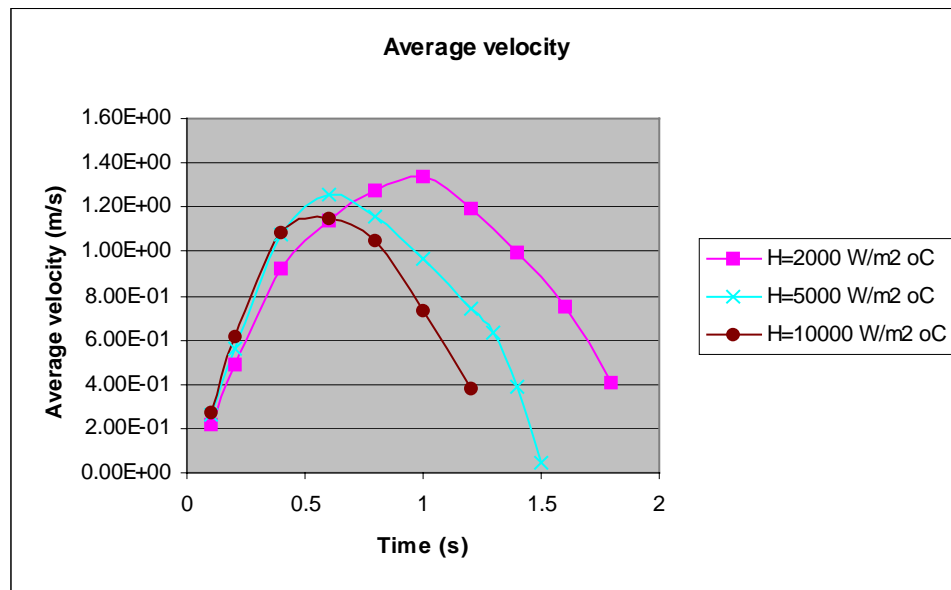


Figure 8. Comparison of average filling velocity for different heat transfer coefficients. Inlet pressure: $P= 20$ kPa; inlet temperature= 1500 °C; mold preheated temperature: $T=400$ °C; phase change temperature: $1400-1410$ °C; mold material: copper

The impact of the convection heat transfer coefficient on the melt solidification process is also studied by using the different convection heat transfer coefficient values of h . The melt solidification process time along with the radial location and the different values of h are shown as follow. When the diameter of solidified melt reaches roughly 25 percent of the outer diameter, the melt is quickly solidified and the flow is stopped. Then the slow cooling process is occurred after this specific time because the conduction is predominant compared to the mixed of convection and convection process before the solidification completed. Figure 9 shows the comparison of solidification front for different heat transfer coefficients. Comparison of solidification process for different mold materials is shown in Figure 10. Figure 11 shows Comparison of average filling velocity for different mold material. Comparison of solidification process for different mold material for $T=800$ °C is shown in Figure 12.

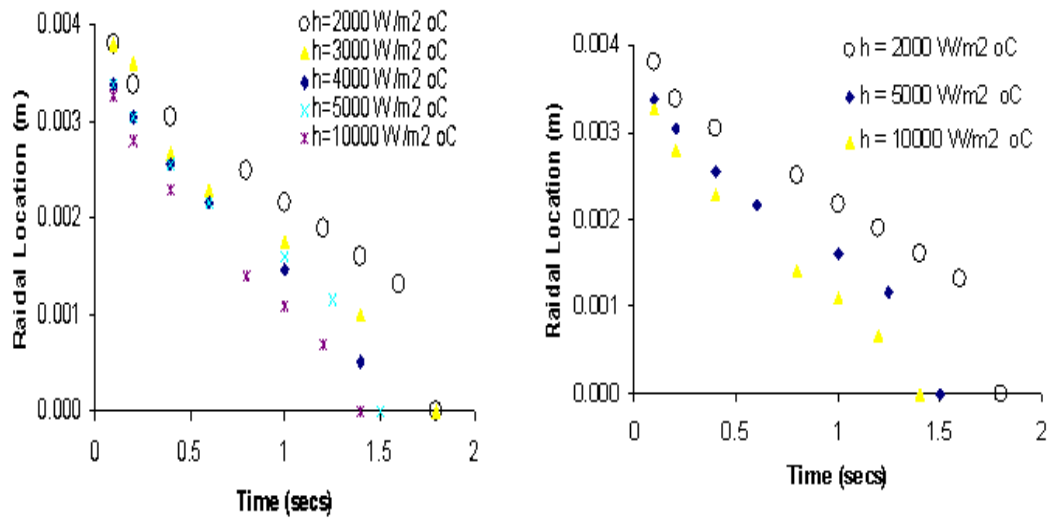


Figure 9. Comparison of solidification front for different heat transfer coefficients.

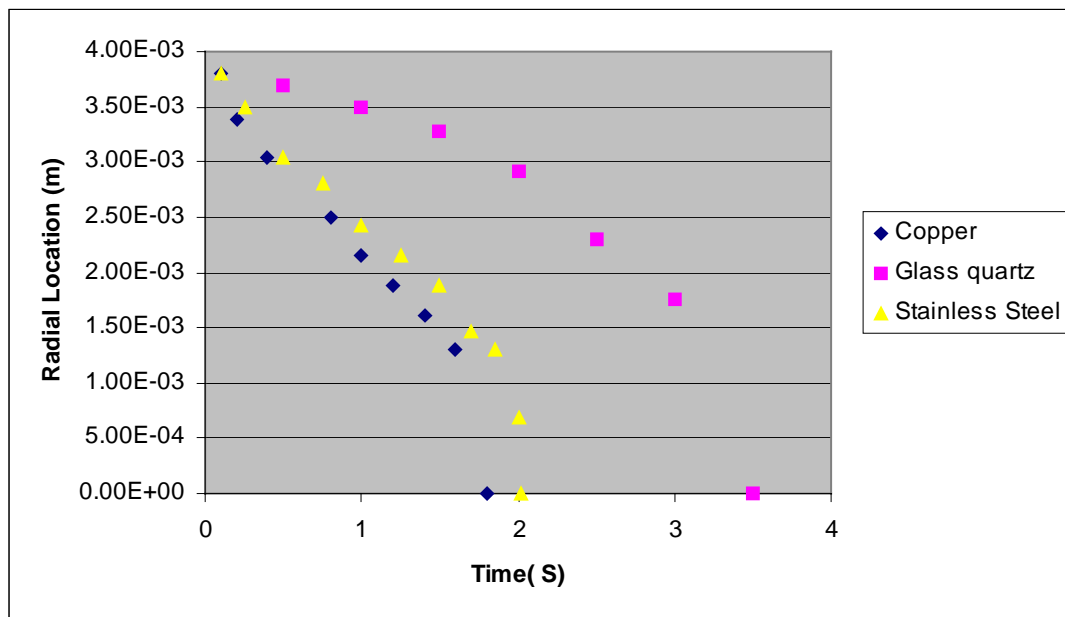


Figure 10. Comparison of solidification process for different mold material
 Boundary conditions and initial conditions: inlet pressure: $P=20$ kPa; inlet temperature= 1500 °C; mold preheated temperature: $T=400$ °C; convection heat transfer coefficient $h=2000$ W/m² °C; phase change temperature: $1400-1410$ °C

At the beginning of the process, the material in the glass quartz mold is solidified slower than that in the stainless steel mold and copper mold. This is because the thermal conductivity of glass quartz is much smaller than copper and stainless steel.

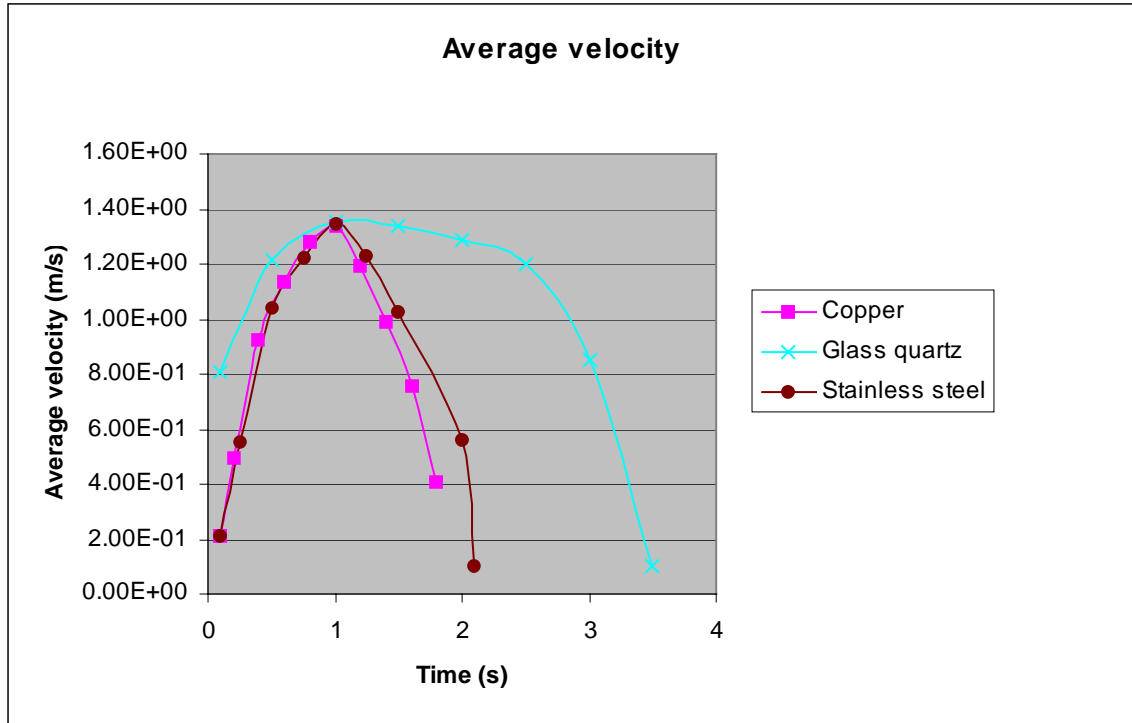


Figure 11. Comparison of average filling velocity for different mold material
 Boundary conditions and initial conditions: inlet pressure: $P= 20 \text{ kPa}$; inlet temperature= $1500 \text{ }^\circ\text{C}$; mold preheated temperature: $T=400 \text{ }^\circ\text{C}$; convection heat transfer coefficient $h=2000 \text{ W/m}^2 \text{ }^\circ\text{C}$; phase change temperature: $1400\text{-}1410 \text{ }^\circ\text{C}$

For the stainless steel mold and copper mold, the average velocity reaches to the maximum velocity and then drops to zero quickly compared to the glass quartz mold. However, for the glass quartz mold, the average velocity reaches to the maximum velocity is slower and it stays at the maximum value range for a longer time, and then drops down slowly. It is because the material of glass quartz has a much smaller value of thermal conductivity than that of copper and stainless steel. It is easy to understand that it takes a longer time for the glass quartz mold for the whole solidification process.

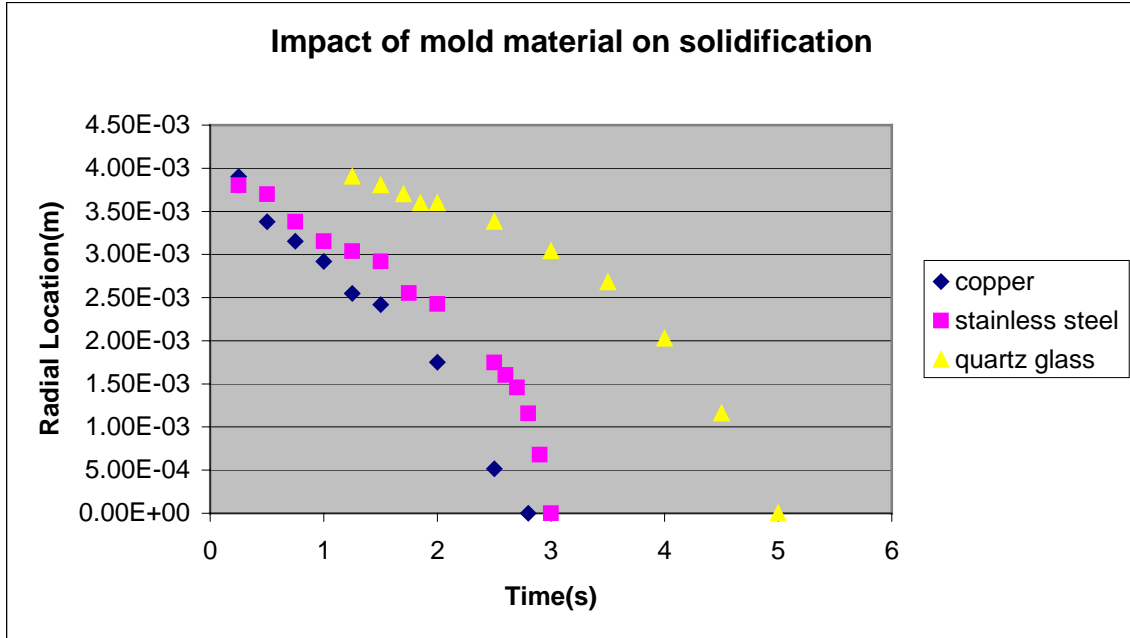


Figure 12. Comparison of solidification process for different mold material
 Boundary conditions and initial conditions: inlet pressure: $P=20\text{ kPa}$; inlet temperature= $1500\text{ }^{\circ}\text{C}$; mold preheated temperature: $T=800\text{ }^{\circ}\text{C}$; convection heat transfer coefficient $h=2000\text{ W/m}^2\text{ }^{\circ}\text{C}$; phase change temperature: $1400\text{-}1410\text{ }^{\circ}\text{C}$

The full paper of "Induction Heating Modeling by a CFD Code" has submitted to the ASME Summer Heat Transfer Conference, Las Vegas, July 20-23, 2003. Paper Number: HT2003-40314.

Mr. Taide Tan has presented "Simulating the Solidification Process in a Melt Casting Metallic Fuel Pin Mold" to the American Nuclear Society (ANS) Student Conference in Berkley, CA, April 2-5, 2003.